[8]G. O. Jones, D. H. Martin, P. A. Mawer, and C. H. Perry, Proc. Roy. Soc. (London) A261, 10 (1961).
[9]G. L. Bottger and A. L. Geddes, J. Chem. Phys. 46, 3000 (1967).
[10]F. C. Brown (private communication of Brandt's results).
[11]F. Bassani, R. S. Knox, and W. B. Fowler, Phys. Rev. 137, A1217 (1965).
[12]F. C. Brown, T. Masumi, and H. H. Tippins, Phys. Chem. Solids 22, 101 (1961); see also F. C. Brown, J. Phys. Chem. 66, 2368 (1962).
[13]B. N. Brockhouse and P. K. Iyengar, Phys. Rev. 111, 747 (1958).
[14]I. Waller and P. O. Froman, Arkiv Fysik 4, 183 (1950).
[15]B. N. Brockhouse, *Inelastic Scattering of Neutrons in Solids and Liquids* (International Atomic Energy Agency, Vienna, 1961), p. 113.
[16]G. Dolling, H. G. Smith, R. M. Nicklow, P. R. Vijayaraghavan, and M. K. Wilkinson, Phys. Rev. 168, 970 (1968).
[17]M. K. Wilkinson, H. G. Smith, W. C. Koehler, R. M. Nicklow, and R. M. Moon, in *Neutron Inelastic Scattering* (International Atomic Energy Agency, Vienna, 1968), Vol. II, p. 253.
[18]G. F. Koster, in *Solid State Physics*, edited by F. Seitz and D. Turnbull (Academic, New York, 1957), Vol. V, p. 173.
[19]R. H. Lyddane, R. G. Sachs, and E. Teller, Phys. Rev. 59, 673 (1941).
[20]H. Cole, J. Appl. Phys. 24, 482 (1953).
[21]W. Cochran, in *Advances in Physics*, edited by F. F. Mott (Taylor and Francis, London, 1961), Vol. 10, p. 401.
[22]G. Gilat and L. J. Raubenheimer, Phys. Rev. 144, 390 (1966).
[23]E. D. Eastman and R. T. Milner, J. Chem. Phys. 1, 444 (1933).
[24]W. T. Berg (private communication).
[25]R. M. Nicklow and R. A. Young, Technical Report No. 3, Office of Naval Research Contract No. NONR 991(00) and 991(06) (unpublished); NR-017-623, Georgia Institute of Technology, Atlanta, Georgia, Project A-389, 1964 (unpublished).
[26]R. P. Lowndes, Phys. Letters 21, 26 (1966).
[27]If Ag is at the origin, the symmetry is L_2'; if Cl is at the origin, the symmetry is L_1.

PHYSICAL REVIEW B VOLUME 1, NUMBER 12 15 JUNE 1970

Photon-Induced Reorientation of Color Centers

R. W. Dreyfus
IBM Thomas J. Watson Research Center, Yorktown Heights, New York 10598
(Received 29 December 1969)

The present experiment investigates the mechanism by which color centers reorient after the absorption of light. In the cases of M and F_A centers in alkali-halide crystals, the F-center portion of a center jumps to an adjacent lattice site after the center has absorbed a (~ 2-eV) photon. From conventional optical measurements, Lüty deduced that the jumping occurs while the F center is in the relaxed excited state. To verify that the reorientation is indeed *not* due to a hot-spot type of phenomenon, the time dependence for the reorientation is measured. That is, the behavior of a color center is analyzed in terms of submicrosecond kinetics. To carry out this measurement, F_A centers are first oriented along a particular axis by illumination with polarized light in the F_{A2} absorption band. The centers are then excited, essentially instantaneously, by Q-switched ruby-laser light. From 0.1 to 10 μsec after the laser flash, the number of centers oriented along each of the cubic axes is measured by the dichroic absorption of polarized F_{A2} light. Thus the reorientation process is followed for times comparable to the lifetime of the excited state. The dichroism of the KBr : F_A(Li) and RbCl : F_A(Na) systems is found to be time dependent. This result confirms the previous deduction that *reorientation occurs by thermally activated jumping* while the F_A center is in the relaxed excited state. An atypically low activation energy, ~ 0.06 eV, allows the jumping to occur rapidly even below 100 °K. The present mechanism also explains the photon-induced reorientation of the M center.

I. INTRODUCTION

A number of color centers in alkali-halide crystals reorient[1] after absorbing an optical photon. Several centers possessing an identifiable axis become preferentially oriented after illumination with polarized light. The M center (which is a pair of F centers on adjacent anion lattice sites) reorients because absorption of a photon stimulates the interchange of one of the F centers with a neighboring host halide ion. This behavior is not unique to the M center, and a general understanding of how a photon produces the interchange is desired.

In the case of the F_A center,[2] Lüty and co-workers deduced the reorientation mechanism from conventional optical measurements.[3] As shown in Fig. 1, the F center has six possible orientations while still remaining a neighbor of the small impurity ion. Each of the six orientations is along a ⟨100⟩ axis.

In discussing the reorientation mechanism it is helpful to visualize the states through which the F_A center goes after absorbing a photon; Fig. 2 shows these states.[3] Photon absorption excites the center from the ground state A to the unrelaxed excited state B, i.e., to upper vibrational sublevels of the excited electronic state. Since the Li^+ neighbor lowers the symmetry from O_h to C_{4v}, the $2p$ excited state separates into $2p_z$ and $2p_{x,y}$ components. The electronic transition moments are no longer isotropic, as Figs. 1 and 2 indicate. In an extremely short time ($\ll 0.001$ μsec) after arrival at B, the F_A center relaxes to state C by the emission of phonons. State C is referred to as the F_A^* center. The F_A^* center in KBr:Li^+ decays to D by spontaneous emission of radiation with a time constant of 1 μsec for $T < 80$°K. Relaxation from $D \rightarrow A$ parallels the relaxation of $B \rightarrow C$. This completes the cycle of absorption, relaxation, emission, and the return to the original state. The question is: At what point in the $A \rightarrow B \rightarrow C \rightarrow D \rightarrow A$ cycle does reorientation occur?

Possible answers to the above question center upon two reorientation mechanisms. The first one is the hot-spot mechanism, which means that the reorientation is activated by the energy released during the relaxation of states $B \rightarrow C$ or $D \rightarrow A$. A temperature dependence only enters into this process through indirect effects such as limiting the mean free path of a phonon or controlling the coupling of upper vibration levels to the lattice phonons. Previous results[4] of polarized luminescence measurements have already eliminated $D \rightarrow A$ as a source of the activation

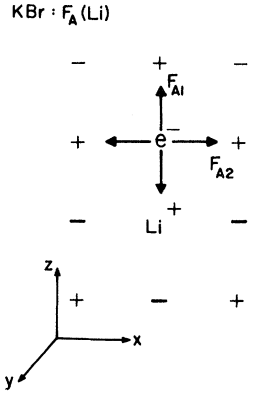

FIG. 1. F_A center in the KBr:LiBr crystal system. The + and − signs represent K^+ and Br^-, respectively. Three other possible F-center locations are shown by heavier − signs. The optical transition moments for the F_{A1} and F_{A2} absorption bands are shown as arrows.

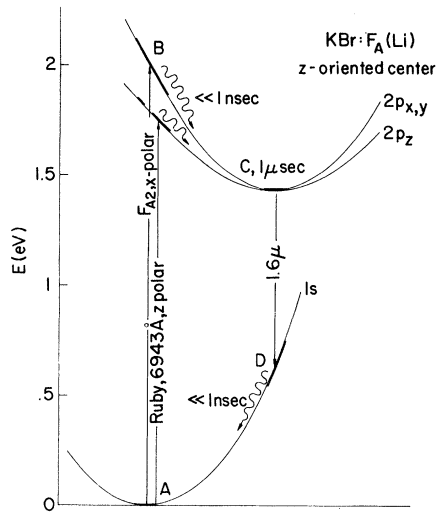

FIG. 2. Conventional configuration coordinate diagram (based on Ref. 4) showing the energy transitions for the F_A center in KBr:LiBr. During the cycle of absorption and fluorescence, the center makes the following transitions: $A \rightarrow B$ represents the optical absorption; $B \rightarrow C$ is due to the relaxation of the ions around the F_A center; $C \rightarrow D$ is the fluorescence transition; and $D \rightarrow A$ is the return to the ground-state configuration. The energy released during the two relaxations, $B \rightarrow C$ and $D \rightarrow A$ would be the source of any hot-spot effects. (This is a schematic representation; the relaxation of $B \rightarrow C$ and $D \rightarrow A$ need not proceed down a parabolic potential as defined by a single variable.)

energy; this leaves only $B \rightarrow C$ to be considered. The hot-spot model is illustrated in Fig. 3(a), where the state of the center now includes its orientation. The energy, nearly $\frac{1}{2}$ eV, released in the $B \rightarrow C$ transition, is viewed as allowing two paths for relaxation, one to C and one to C'. The branching ratio for these two paths is defined as α. The α would need to be temperature dependent in order to agree with the previous quantum-efficiency results,[4] which showed a temperature dependence. After reaching C or C', the center would decay to the respective ground states, i.e., $C \rightarrow D \rightarrow A$ or $C' \rightarrow D' \rightarrow A'$.

The second model which can explain the reorientation behavior is based upon a conventional atom jump, the same motion that occurs in diffusion processes. In this case, reorientation is activated directly by the thermal energy of the lattice. This diffusion model has reorientation occurring while the F_A center is in state C, see Fig. 3(b). During the 1-μ sec lifetime of state C, reorientation can occur at low temperatures if this state results in an atypically small jump energy (~0.1 eV). The ground state A is already known to have a reorientation activation energy of ~1 eV. [This direct $A \rightarrow A'$ jump is not shown in Fig. 3(b) since this

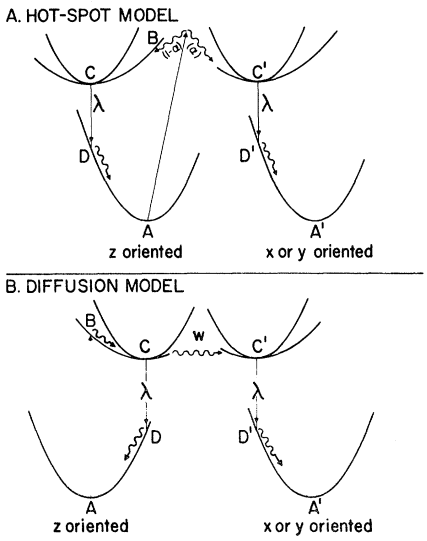

FIG. 3. Extension of Fig. 2 to show the two possible mechanisms responsible for the reorientation of the F_A center. The present diagram therefore incorporates levels for unrotated centers, i.e., z-axis oriented both before and after excitation, as well as levels for reoriented centers, i.e., those lying finally along x or y axes. The centers all start from state A; the electronic states associated with the reoriented centers are designated by primed letters. In the case of the hot-spot model, upper diagram, the reorientation is essentially part of the excitation phenomenon; the reorientation probability is controlled by a branching ratio $\alpha(T)$. In the diffusion model, lower diagram, the reorientation occurs as a thermally activated atomic jump with rate constant $w(T)$. This jump is shown as going from $C \rightarrow C'$; however, the back reaction, $C' \rightarrow C$, is subsequently possible.

jump has a negligible probability per second for temperatures of present interest, i.e., $T < 100\,^{\circ}\mathrm{K}$.] Such a great difference in reorientation energy between A and C would be surprising. Experimentally, however, the classical optical measurements of Lüty *et al.* did lead them to this diffusion mechanism.[3,4] A complex series of experiments was required to arrive at this conclusion.

To check this conclusion, the author has investigated the reorientation mechanism using a completely different experimental approach. This new approach measures the concentration of F_A centers in different orientations as a function of time (μsec) after excitation. To determine the time dependence, one must know the exact moment of excitation; this is established by exciting all the F_A centers simultaneously with a Q-switched ruby laser.

The present experiment involves illuminating the sample with different intensities and wavelengths of light as follows:

(i) The sample is illuminated in the F_{A2} band with vertically polarized light, thereby orienting the F_A centers vertically. The vertical axis of the laboratory is taken to be the z axis throughout the following discussion. Figure 2 implies that vertically polarized F_{A2} light is not absorbed by z oriented centers but only by x and y oriented centers. (To illustrate this point in detail, Fig. 2 would have to be also drawn for centers oriented along x and y axes.) Since only x and y oriented centers absorb vertically polarized F_{A2} light, only these orientations are stimulated to reorient during the present step of the experimental procedure. On a statistical basis nearly all the centers will settle down into the $\pm z$ orientation after several excitations. Since this step is carried out with a conventional light source, alignment of the centers requires several minutes. This time contrasts markedly with the next two steps, which require only μsec.

(ii) A Q-switched ruby laser flashes for a period of 0.07 μsec and excites the centers via the F_{A1} absorption band. The excitation may be considered as instantaneous, because the laser is on for much less than the fluorescence time (1 μsec) of the F_A^* center. The time of the laser flash is defined as $t = 0$.

(iii) The reorientation kinetics are then followed by measuring the absorption in the F_{A2} band. From t equal to -0.1 to 10 μsec the absorption of either vertically (z) or horizontally (x) polarized light is recorded. The optical density is proportional to the instantaneous concentration of F_A centers oriented so that they can absorb the polarized F_{A2} light. This means that the present optical density measurements provide values for the concentration of centers in states A and A' (see Fig. 3) as a function of time. The F_A^* centers do not absorb in the visible range. Section II shows how this time-dependent absorption differentiates between the hot-spot and diffusion mechanisms of reorientation.

II. THEORY

The quantitative expressions used to interpret the observed reorientation kinetics are derived in two steps. First, the time dependences are derived for the populations of complexes in particular orientations. Second, the time-dependent absorption of polarized light is related to these populations of complexes in specific orientations.

Hot-spot model. This model is analyzed first because it is both simple and exemplary. Figure 3(a) shows the nature of the hot-spot mechanism; note that state C' is filled in coincidence with the light absorption. This does not imply that the absorption process always results in the center

arriving at C', rather the branching ratio α relates the probability of filling C' as compared to C. The time-dependent concentration of centers in each state is indicated by the letter n with an appropriate subscript, e.g., $n_{C'}$. Also, it should be noted that n refers to the concentration in a particular direction or orientation, such as the $-x$ direction. After the initial relaxation of $B \rightarrow C$, the total concentration of centers N is $2n_A + 4n_{A'} + 2n_C + 4n_{C'}$.

The differential equations linking n_C and $n_{C'}$ to the spontaneous fluorescence rate λ are

$$dn_C/dt = -\lambda n_C, \quad dn_{C'}/dt = -\lambda n_{C'} . \tag{1}$$

The solutions to (1) are

$$n_C = \tfrac{1}{2}N(1-4\alpha)\exp(-\lambda t), \quad n_{C'} = \alpha N \exp(-\lambda t). \tag{2}$$

The constants appearing in (2) reflect the initial conditions: All the F_A centers are in state A before excitation, and the probability of reorientation is proportional to the branching ratio α.

Integration relates the concentrations of light-absorbing centers A and A', to Eq. (2)

$$\begin{aligned} n^f_{A'} - n_{A'}(t) &= \int_0^\infty \lambda n_{C'}\, dt - \int_0^t \lambda n_{C'}\, dt \\ &= \int_t^\infty \lambda n_{C'}\, dt = \alpha N \exp(-\lambda t), \\ n^f_A - n_A(t) &= \int_t^\infty \lambda n_C\, dt = \tfrac{1}{2}N(1-4\alpha)\exp(-\lambda t). \end{aligned} \tag{3}$$

The superscript f indicates the concentrations after all centers have returned to their ground states, i.e., final states.

Next the intensity of the transmitted light is related to the above concentrations of centers. The experimental data are expressed as an intensity ratio $i(t)$ where $i(t) = I(t)/I^f$. $I(t)$ is the intensity of polarized F_{A2} light passing through the sample as a function of time, and I^f is the (final) intensity after all the F_A centers have returned to their ground states. Including a specification of the polarization for $i(t)$, the resultant quantities are related to the concentrations of centers

$$\begin{aligned} \ln i_z(t) &= 4\sigma l[-n_{A'}(t) + n^f_{A'}], \\ \ln i_x(t) &= 2\sigma l[\, n^f_A - n_A(t) + n^f_{A'} - n_{A'}(t)], \end{aligned} \tag{4}$$

where σ is the cross section for absorption of F_{A2} light and l is the sample length. The first equation links i_z to the x and y oriented centers, because the F_{A2} transition moment is perpendicular to the axis of the F_A center. The same relationship means that the absorption of x-polarized light is related to the concentration of centers pointing in the y and z directions. Consequently, both primed (y orientation) factors and unprimed (z orientation) factors appear in the second equation. Combining Eqs. (3) and (4) gives

$$\ln i_z = 4\sigma l N \alpha \exp(-\lambda t), \tag{5}$$

$$\ln i_x = \sigma l N(1-2\alpha)\exp(-\lambda t). \tag{6}$$

This pair of equations illustrates the basic point that $i_x(t) \neq i_z(t)$ if the reorientation takes place by the hot-spot mechanism. In Sec. III, this inequality is checked on a plot of log log i_z and log log i_x versus t, in which case Eqs. (5) and (6) predict parallel nonintersecting lines. [The trivial case of complete coincidence of (5) and (6) is avoided by making measurements at a sufficiently low temperature that $\alpha < \frac{1}{6}$.]

The following combination of (5) and (6) provides one expression for the dichroism

$$\frac{\ln i_x - \ln i_z}{\ln i_x + \frac{1}{2}\ln i_z} = 1 - 6\alpha . \tag{7}$$

Equation (13) will bring out the importance of this specific relationship. For the present it is sufficient to note that the right-hand side of (7) is independent of t.

Diffusion model. Figure 3(b) shows the path by which the ground states are filled when the reorientation takes place by a diffusion type of jump from one excited state to a differently oriented one. The differential equations for the concentrations in the excited states are now

$$\begin{aligned} \frac{dn_C}{dt} &= -n_C(4w+\lambda) + 4w n_{C'} , \\ \frac{dn_{C'}}{dt} &= -n_{C'}(2w+\lambda) + 2w n_C . \end{aligned} \tag{8}$$

Equation (8) shows that C' is filled from C (not A as in the hot-spot model), and that the rate factor for this filling is w for jumps in a particular direction. The value of w should be temperature dependent according to the usual Arrhenius equation [given later as Eq. (14)], although this is a point to be checked. The possibility of the subsequent $C' \rightarrow C$ back reaction is included in (8). The factor λ is still the rate constant for deexcitation to the ground state. The differences between (1) and (8) give rise to the different time dependences between the diffusion and hot-spot models.

The solutions of (8) are

$$n_C = (1 + 2\, e^{-6wt})\tfrac{1}{6}N e^{-\lambda t} , \quad n_{C'} = (1 - e^{-6wt})\tfrac{1}{6}N e^{-\lambda t} . \tag{9}$$

The concentrations in the ground states are again obtained by integration, with the results that

$$\begin{aligned} n^f_A - n_A &= \left[1 + \frac{2\lambda \exp(-6wt)}{\lambda + 6w}\right]\tfrac{1}{6}N e^{-\lambda t} , \\ n^f_{A'} - n_{A'} &= \left[1 - \frac{\lambda \exp(-6wt)}{\lambda + 6w}\right]\tfrac{1}{6}N e^{-\lambda t} . \end{aligned} \tag{10}$$

The intensity of light passing through the sample is still given by (3); for the diffusion model

the solution is

$$\ln i_z = \tfrac{2}{3}\sigma l N\left[1-\frac{\lambda\exp(-6wt)}{\lambda+6w}\right]e^{-\lambda t},$$

$$\ln i_x = \tfrac{1}{3}\sigma l N\left[2+\frac{\lambda\exp(-6wt)}{\lambda+6w}\right]e^{-\lambda t}. \qquad (11)$$

In Eq. (11) $i_z \neq i_x$ for $6wt < 1$, but $i_z \approx i_x$ for $6wt > 2$. Thus i_x and i_z start out being unequal and at a later time $t < 2/6w$ can become (approximately) equal.

This transition occurs only in the diffusion model and, consequently, serves to differentiate the diffusion model from the hot-spot model.

The above equations are solved for the exponential time dependences $-6wt$ and $-\lambda t$

$$\sigma l N e^{-\lambda t} = \ln i_x + \tfrac{1}{2}\ln i_z, \qquad (12)$$

$$\frac{\lambda}{\lambda+6w}e^{-6wt} = \frac{\ln i_x - \ln i_z}{\ln i_x + \frac{1}{2}\ln i_z}. \qquad (13)$$

Equation (13) shows that a plot of the right-hand side (on a log scale versus t) establishes w from the measured intensities.

III. EXPERIMENTAL TECHNIQUE

The present experiment determines the kinetics of the reorientation process from dichroism measurements. As shown in Sec. II, a detailed knowledge of these kinetics is sufficient to differentiate between the two models. The equipment used for these measurements is shown in Fig. 4.

The first step is to align the F_A centers along the z axis by illumination with z-polarized F_{A2} light (i.e., light of 6000 to 6300 Å wavelength for the present crystal systems). The light source consists of a microscope illuminator placed between the concave mirror and the narrow-pass optical filter (see Fig. 4).

The second step involves illuminating the sample with a Q-switched ruby laser. Timing, i.e., $t = 0$, is established by having the laser flash also trigger the oscilloscope sweep circuit via a photodiode. The laser flash lasts 0.07 μsec and has a flux density of 10^{18} photons/cm^2. The flash increases the sample temperature less than 0.01 °K.

The flashlamp which excites the ruby laser also supplies the F_{A2} light for step 3 of the measurement. Step 3 is the recording (for 10 μsec following step 2) of the time-dependent transmission of polarized F_{A2} light. For this short time period, the flashlamp intensity remains practically constant. The F_{A2} light intensity is recorded on a dual-beam oscilloscope.[5] The lower trace displays the rapidly changing high-intensity light in the $0 < t < 1$- μsec period; the upper trace displays the asymptotic approach to the final light levels on an expanded scale, primarily for $1 < t < 10$ μsec. Shot noise in the photomultiplier plus an allowance for nonlinearities in the oscilloscope display produce the error limits shown later in Fig. 6(b).

The above three steps are repeated twice at each temperature. The difference between the two cycles is that the axis of the polarizer is rotated from the vertical to the horizontal position for step 3 of the second cycle. Thus the first time through gives the value of $i_z(t)$ and the second time gives $i_x(t)$. The present technique of normalizing these intensities means that differences in flashlamp intensities between two flashes will not influence the experimental results.

The sample is mounted on a copper block within a Cryojet (Magnion Corp., Burlington, Mass.) cooling unit; flowing liquid nitrogen is the coolant. The gas pressure over the liquid nitrogen can be lowered in order to reach temperatures as low as 64 °K.

To produce F_A centers, ingots are grown from melts of the following compositions: KBr: (1%) LiBr and RbCl: (1%) NaCl. Crystals cleaved from the ingots are colored by the well-known van Doorn technique.[6] With the crystal near 0 °C, the F cen-

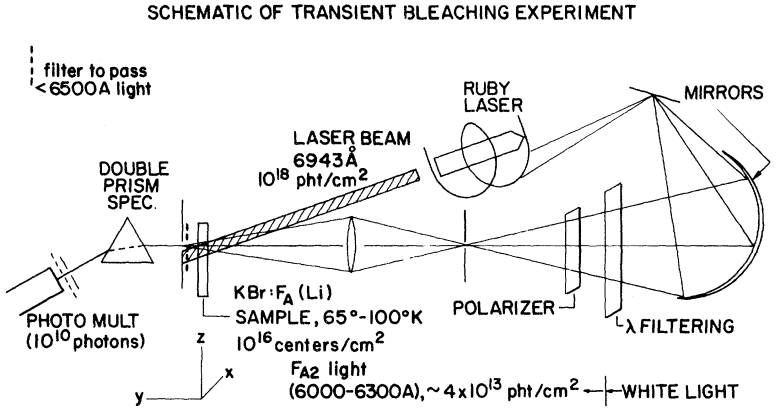

FIG. 4. A schematic representation of the present optical equipment. Note that the photomultiplier measures the intensity of the F_{A2} light transmitted by the sample. The source of this F_{A2} light is the flashlamp, which also excites the ruby-laser rod. The λ filtering is a conventional narrow-pass interference filter. The spectrometer passes the same wavelength as this filter. Surrounding the sample is a vacuum cryostat; this item is not shown.

ters are converted to F_A centers by a 1-h exposure to sodium light (5890 Å).[7] Immediately thereafter, the samples are cooled to the liquid-nitrogen temperature range and remain there for the duration of the measurements. F_A-center concentrations are kept low (near 10^{16} cm^{-3}) in order to minimize high-concentration effects, such as have been studied in KI:(10^{17} to 10^{18}cm^{-3})F by Fröhlich and Mahr.[8]

IV. EXPERIMENTAL RESULTS

Figure 5 shows examples of the (x and z) polarized light transmission for three temperatures. In Fig. 5, the data points for 74.6° are particularly important. These points reflect the presence of two effects. The over-all trend is for i_x and i_z to decrease with time owing to the depopulation of the excited state by spontaneous emission of radiation, i.e., fluorescence. The fact that fluorescence increases the absorption results from the ground state being the only one capable of absorbing F_{A2} light. Besides the temporary increase in i_x and i_z, the difference between these two directions of polarization is also evident, i.e., dichroism is present. At 74.6° the dichroism lasts for nearly 1 μsec; thereafter, the data points are coincident. Recall that dichroism indicates a difference in concentration between the two orientations (z versus x, y) of F_A centers. The concentration difference is therefore disappearing in a time of ~1 μsec. The hot spot is dissipated in a time <0.001 μsec, since it involves the (rapid) ballistic emission of lattice phonons. Consequently, the reorientation must be occurring by a much slower process, namely, *the diffusion mechanism*. This conclusion is a rephrasing of Sec. II, i.e., had the hot-spot mechanism been the correct one, then the intensity curves would either have been parallel or completely coincident, but never convergent.

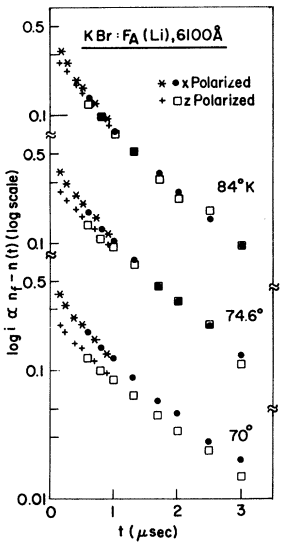

FIG. 5. The normalized transmitted intensity versus time for three sample temperatures. The experimental uncertainty is not shown until Fig. 6 because it is negligible on the present scale and only becomes apparent when i_z is subtracted from i_x. Laser excitation occurs at $t=0$. The use of two symbols for each polarization indicates which of the two oscilloscope beams displayed the data. The negative slope of ~ -1 (as drawn) is due to deexcitation via emission of 1.6-μ radiation. The primary point of interest is the difference in absorption for the two directions of polarization, i.e., dichroic absorption of light. Dichroism indicates a net alignment of F_A centers along the z axis.

A qualitative look will now be taken at the effect of temperature upon the time required for i_x and i_z to converge. Subsequently, the data will be analyzed in terms of Eq. (13) of Sec. II.

In Fig. 5, the 70°K data points indicate dichroism even out to 3 μsec. Consequently, the F_A^* center is returning to the ground state before reorientation takes place, i.e., $6w << \lambda$. That low temperature should produce this situation is reasonable, since the probability of reorientation,[9] η_R, and consequently, w decrease rapidly as the temperature decreases. On the other hand, λ is essentially independent of temperature in the present range.[10]

The 84°K data points in Fig. 5 indicate very little dichroism; only the points at 0.15 and 0.25 μsec show a significant difference in intensity with polarization. Thus 84° is sufficiently high for rapid ($t < 0.5$ μsec) reorientation to take place when the center is in the excited state. Again this agrees with the classical measurements,[9] which show that 84° is sufficient to produce randomization with high-quantum efficiency. Referring to Fig. 3(b), the situation is now $6w > \lambda$.

The next step is to analyze the data in terms of Eq. (13); this equation determines the value of w from the measured quantities i_x and i_z. Figure 6 illustrates the way this is carried out. In Fig. 6(a) the normalized intensity appears as a function of t for both polarizations. The intensity points for each time are then combined according to the right-hand side of Eq. (13); this provides a series of values for $\lambda(\lambda + 6w)^{-1}\exp(-6wt)$. The logarithm of this quantity is plotted versus t in Fig. 6(b); the slope indicates the value of w for 74.6°.

Values of w are determined for many temperatures between 65° and 95°; the results are plotted as log$w$ versus T^{-1} in Fig. 7. The fact that the points in Fig. 7 follow a straight line (within experimental uncertainty) indicates w fits the Ar-

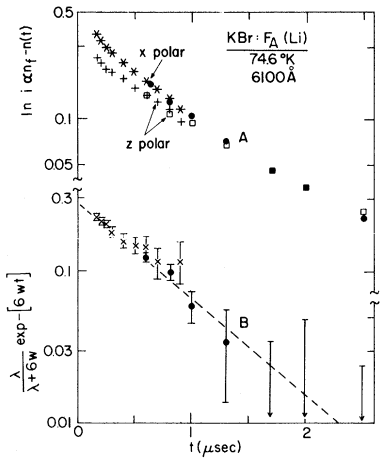

FIG. 6. Data analysis using the 74.6° points from Fig. 5. In part A the scales are magnified in order to make the dichroism more easily observed. The points in B are obtained by inserting the intensities for each time into Eq. (13). The slope in B provides the experimental value for the reorientation rate w. The experimental uncertainty is primarily produced by the shot noise in the photomultiplier signal, i.e., in the observed values of i.

rhenius equation

$$w = w_0 e^{-\epsilon/kT} \quad . \tag{14}$$

The activation energy ϵ is the energy for the jumping atom to go from the lattice site to the (energy) saddle-point position which exists halfway between lattice sites. The quantity w_0 is the frequency with which the atom attempts to overcome the saddle-point barrier. The applicability of (14) to the present data provides further evidence that the diffusion model is correct, since essentially all atomic jump rates follow this equation.

Two cross checks have been made on the present experiment. First, two different wavelengths (6100 and 6300 Å) of light have been used in step 3 of the measurement. Figure 7 shows that the measured value of w is independent of which wavelength is utilized (both wavelengths lie within the F_{A2} band). This independence indicates that, as anticipated, the F_{A2} band is the only one undergoing relaxation in step 3 of the measurement.

The second cross check involves substituting RbCl: F_A(Na) for KBr: F_A(Li) in order to show that the latter system is not unique in its behavior. The time-dependent disappearance of dichroism for this other system exactly parallels that shown in Fig. 5. The results for log$w$ versus T^{-1} are shown in Fig. 8 for the RbCl: F_A(Na) system. The only difference is that given values of w are displaced to temperatures about 10° higher, again in agreement with Ref. 9. The similar behavior observed for the two systems leads one to believe that the diffusion model is applicable to all the thermally activated F_A^* reorientations, that is, to the behavior of so-called[3,4] F_A(I) centers. The present measurements do not directly provide information about temperature-independent reorientations, i.e., reorientations of F_A (II) centers such as KCl: F_A(Li).

V. DISCUSSION

The present data in Figs. 7 and 8 indicate ϵ values of 0.085 ± 0.025 and 0.06 ± 0.015 eV, respectively, while $w_0 = 7\times10^{10}$ sec^{-1} and 3×10^{8} sec^{-1}. The unusual feature of these energies is that they are only 10% of the diffusion (reorientation) energy without photon excitation. (The ground-state reorientation energy is near 1 eV.[3]) The Appendix indicates the probable reason for this reduction in activation energy. Along with these small values of ϵ, one notes that w_0 is several decades smaller than values usually found in diffusion measure-

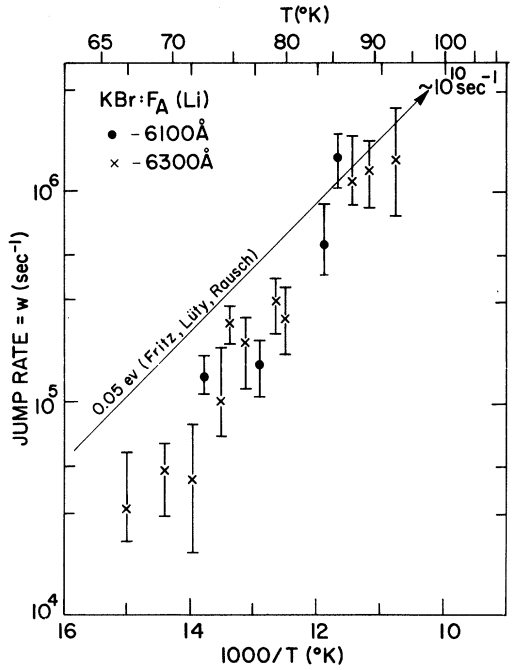

FIG. 7. Values of the reorientation rate w versus T^{-1} plotted according to the Arrhenius equation. The data from the present laser excitation technique are shown as x and •. The two different symbols indicate the two different wavelengths of F_{A2} light used in the present experiment. As is anticipated, the present results are not affected by this change. The experimental uncertainty involves the question of measuring slopes, such as appear in Fig. 6(b). The solid line is obtained from the classical optical data of Fritz, Lüty, and Rausch,[4] by means of Eq. (15). The present data points indicate an activation energy ϵ equal to 0.085 ± 0.025 eV and a frequency factor w_0 of 7×10^{10} sec^{-1}.

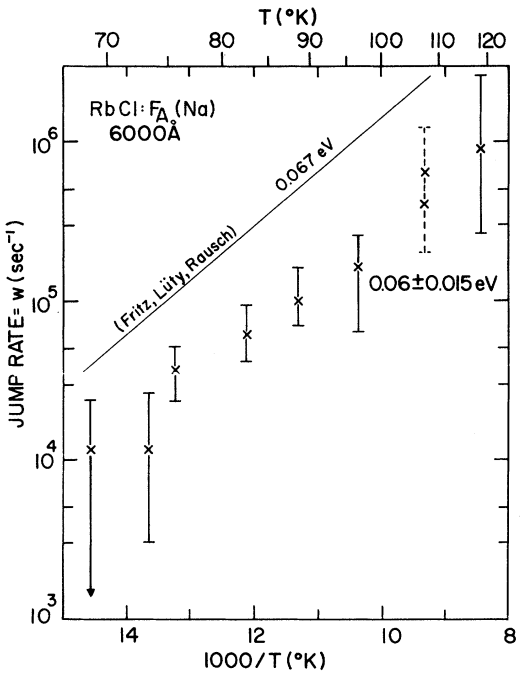

FIG. 8. Similar to Fig. 7, except now for the RbCl: F_A(Na) system. In this case $\epsilon = 0.06 \pm 0.015$ eV and $w_0 \approx 3\times10^8$ sec^{-1}.

ments. This reduction in w_0 is due to the relatively small restoring force ($\propto \epsilon$) tending to hold the F_A^* center at the lattice point.

A comparison can be made between the present values of $w(T)$ and the values of $w(T)$ from the previous optical measurements. The previous results were expressed in terms of $\eta_R(T)$, the quantum efficiency for reorientation.[4] Expressing η_R in present terms $\eta_R = 4n_A^f/N$. Since $n_{A'}(t=0)$, Eq. (10) provides a relation between $n_{A'}^f$ and w

$$n_A^f = n_{A'}^f - n_{A'}(t=0) = Nw/\lambda + 6w .$$

Solving for w gives

$$w = \lambda/-6+4\eta_R^{-1} . \qquad (15)$$

This equation is used to transform the data of Ref. 9 into the solid lines in Figs. 7 and 8. The previous results are noted to be up to 50% larger than the present values of w. It is the present conclusion that the difference primarily lies in the measurement of temperature and not in the different techniques of measuring w. This is based upon attempts to reproduce the previous results[9] but with the present apparatus. The present finding is a lower value for η_R, primarily for $T < 75\,^\circ$K. In other words, the present experimental arrangement indicates a temperature $\sim 5^\circ$ higher than previously found for a given value of η_R. This is not a serious disagreement, however, when one compares it to the significant areas of agreement between the two completely different experiments. Agreement covers the following points: (a) The reorientation is due to a diffusion type of atom jump while the center is in the F_A^* state; (b) the reorientation rate is controlled by the Arrhenius equation; and (c) two completely different experiments agree within 50% for the jumping rate in the excited state. It should be recalled that these jumping rates are for a state whose lifetime is ≤ 1 μsec.

ACKNOWLEDGMENTS

Aid in preparing the samples and assembling the equipment was supplied by R. Linn. Discussion with F. Lüty and J. Armstrong is gratefully acknowledged.

APPENDIX: REORIENTATION OF M^* CENTER

A subsidiary point to be considered is whether the diffusion model explains the reorientation properties of the M^* center. For the F_A^* center the present work confirms that rapid atomic jumping occurs because the excited-state electronic configuration reduces ϵ the saddle-point energy. With respect to the reason for this reduction, Lüty[11] suggests that the orientational properties of the $2p_{x,y}$ excited states produce the low value of ϵ. (Note that *orientational properties* means orientation of electronic wave functions in the present context.) Specifically the $2p_{x,y}$ states orient so that the maximum electron density centers on the (unoccupied) anion lattice sites when the jumping anion is at the saddle point. Vacant anion sites produce a virtual positive charge and hence attract the electron cloud. The Coulombic interaction of the electron cloud with the virtual positive charge then reduces the energy of the saddle point. (The F_A ground state is a symmetrical $1s$ configuration; consequently, this state is not significantly perturbed by the anion going from the equilibrium to the saddle-point configuration.)

The question of whether M^* reorientation is also interpretable in terms of the above model then becomes a question of whether $2p_{x,y}$ states lower the saddle-point energy for the M^* center as they did for the F_A^* center. *Note added in proof.* Since submission of the present paper, I. Schneider [Bull. Am. Phys. Soc. 15, 340 (1970)] suggested that the reorientation of the M center primarily occurs as a result of ionization of the M center, i.e., the M^+ center actually is the reorienting species. Even though the M^+ center possesses π_u and σ_u excited states somewhat similar to the M center, the exact role of each state has not yet

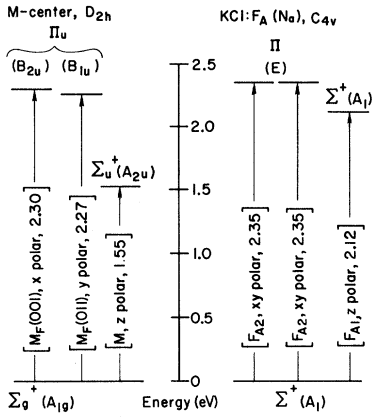

FIG. 9. Comparison of the energy levels for the M center (Ref. 1) and F_A center (Ref. 4) in KCl. The levels are labeled according to molecular orbital terminology, which is equivalent to considering each color center as a diatomic molecule and the rest of the lattice as a homogeneous dielectric medium. The specific wave-function symmetry is given in the parenthesis after each molecular wave-function designation. The molecular wave functions for the F_A center are based on the F_A center being a heteronuclear diatomic molecule, see Hertzberg, *Spectra of Diatomic Molecules* (Van Nostrand, Princeton, N. J., 1967), p. 318. The Π states in Fig. 9 are equivalent to the $2p_{x,y}$ states in Figs. 2 and 3. With the exception that parity is not appropriate with respect to the F_A center, the molecular wave functions of the M center have the same symmetry as the F_A center wave functions. Furthermore, the energy levels are similarly spaced. The optical absorption transitions are shown as vertical arrows. The [ ] in the arrows show common terminology for the transition, transition moment, and energy in eV, respectively.

been made explicit. The above work thus interjects a question into the discussion of whether the present F_A^* results are applicable to a detailed analysis of the M^* reorientation. On the other hand, ionization of the F_A center does not enhance the reorientation of the F_A center. This is based upon the observation that electric field ionization hinders reorientation of the F_A center (Ref. 3, Figs. 3–18). The above reference to M-center behavior consequently does not directly influence the present deduction that F_A^*-center reorientation is due to a diffusion type of jump in the relaxed excited state. The comparison of M^* and F_A^* centers is best made in terms of molecular quantum states, because then the resonant interaction is correctly included for the two F centers which make up the M center. Figure 9 gives the term assignments and energy levels for both M and F_A centers; it is immediately evident that significant similarity exists between the two centers. Particularly in the case of the M center it should be noted that the transition moments from the ground state to the Π states are all in the xy plane, i.e., perpendicular to the axis of the color center.[1] This means that the Π-state wave functions are similar to the $2p_{x,y}$ wave function of the F_A^* center. Furthermore, these are exactly the electronic wave wave functions which can orient so as to lower the saddle-point energy by means of the Coulombic interaction. Thus the low value of ϵ for the M^* center can be readily interpreted as a Coulombic interaction involving $\Pi(2p_{x,y})$ states similar to the explanation previously put forth concerning the F_A center.

The proof of the similar reorientation mechanisms actually goes further. In the case of the M^* center, reorientation does not occur at 77 °K if the Σ_u state is excited.[1] This means that the z oriented wave function of the Σ_u state is incapable of producing the required lowering of ϵ. Hence only the Π_u wave functions are appropriately oriented to overlap the vacant anion sites and thereby reduce the value of ϵ through a Coulombic interaction. One is not able to ascribe the lowering of ϵ to a particular wave function in the F_A^*-center work, because the Σ state (of the F_A^*) overlaps the Π state, and properties can not be uniquely ascribed to either. The results from reorientation properties of M^* centers thus provide direct evidence for the importance of the Π_u $(2p_{x,y})$ states.

---

[1]C. Z. van Doorn and Y. Haven, Phys. Rev. 100, 752 (1955); T. J. Turner, R. De Batist, and Y. Haven, Phys. Status Solidi 11, 267 (1965); 11, 535 (1965).

[2]The F_A center is an F center bound to a small monovalent metal impurity within the alkali-halide lattice. F centers bound to Li^+ in KBr are primarily studied in the present work and are referred to as KBr:F_A(Li). The F-center portion of the F_A center will retain its name for purposes of present discussion.

[3]F. Lüty, *Physics of Color Centers*, edited by W. B. Fowler (Academic, New York, 1968), Chap. 3.

[4]B. Fritz, F. Lüty, and S. Rausch, Phys. Status Solidi 11, 635 (1965).

[5]Tektronix model 556. The 556 oscilloscope contains an 0.1-μsec time delay in the vertical amplifier; consequently, the vertical display starts at $t = -0.1$ μsec. This means the transmission of the sample is recorded in the before-excitation state. The difference between this transmission and the transmission after ~ 10 μsec allows one to calculate the quantum efficiency for reorientation. This calculation is utilized in Sec. V.

[6]C. Z. van Doorn, Rev. Sci. Instr. 32, 755 (1961).

[7]The general method of producing F_A centers is described by H. Hartel and F. Lüty, Z. Physik 177, 369 (1964). The present temperatures and wavelengths are selected to maximize the production rates in the present crystal systems.

[8]D. Frölich and H. Mahr, Phys. Rev. 148, 868 (1966).

[9]Figure 6(b) of Ref. 4.

[10]G. Spinolo and F. C. Brown, Phys. Rev. 135, A450 (1964).

[11]Reference 3, pp. 228–236.

PHYSICAL REVIEW B VOLUME 1, NUMBER 12 15 JUNE 1970

Theory of Light Scattering from Polaritons in the Presence of Lattice Damping

H. J. Benson and D. L. Mills†
Department of Physics, University of California, Irvine, Irvine, California 92664
(Received 9 February 1970)

We formulate the theory of light scattering from polaritons in ionic crystals by a Green's-function method. The theory is presented in a form that allows the effect of the damping of the lattice motion to be included in a rigorous fashion. Difficulties encountered in earlier phenomenological approaches to the problem are eliminated by the present work. It is pointed out that, in principle, detailed studies of the shape of the Raman line may be utilized to determine the frequency dependence of the phonon proper self-energy over a wide range of frequencies. We present the results of numerical studies of the shape and position of the Raman line as a function of scattering angle, for the case where the frequency dependence of the proper self-energy is ignored. We find that even when the damping of the lattice is appreciable, the position of the line center as a function of scattering angle is given accurately by employing the polariton dispersion relation appropriate to the case where *no* damping is present.

I. INTRODUCTION

The transverse optic (TO) phonons of long wavelength generate a macroscopic electromagnetic (EM) wave when they are excited. As a consequence, the long-wavelength normal modes of an ionic crystal are mixed modes, involving both lattice motion and the EM field. These mixed modes are called "polaritons." The study of the Raman scattering of light from these modes has provided useful information about the properties of polaritons, and a number of other properties of ionic crystals.[1] Since the polariton modes contain roughly an equal admixture of lattice motion and EM field when the wave number q of the polariton is near ω_{TO}/c, where ω_{TO} and c are the frequency of the TO phonon and the velocity of light, experimental study of these modes requires observation of the Raman effect in the near forward direction. This is because ω_{TO}/c is small compared to the wave vector of light employed in these experiments.

The theory of the Raman scattering from polaritons was first discussed by Loudon.[2] In many discussions of the experimental data, one ignores the effect of the damping of the lattice motion on the spectrum of the scattered light. One then obtains a line that has zero width, i.e., the radiation leaving the crystal contains spectral components at $\pm\omega_\pi(\vec{q})$, where $\omega_\pi(\vec{q})$ is the polariton frequency appropriate to the particular scattering angle examined. In real crystals, the lattice motion is damped, either by anharmonic effects or by crystal imperfections. The finite lifetime of the TO phonon will cause the spectral distribution to scattered light to be spread out in frequency, and will also shift the position of the center of the Raman line. The purpose of this paper is to present a theory of the line shape and frequency shift, and to discuss the kind of information one may obtain by studying these quantities.

A phenomenological means of describing the position of the line center has appeared in a number of papers.[3] In the absence of any damping, the polariton dispersion relation may be written in the form

$$c^2q^2/\omega^2 = \epsilon(\omega) = \epsilon_0 + 4\pi\beta\omega_{TO}^2/(\omega_{TO}^2 - \omega^2) \ , \qquad (1)$$

where ϵ_0 is the high-frequency (optical) dielectric constant, and β is the contribution of the lattice to the static polarizability of the crystal. Polariton dispersion curves computed for parameters appropriate to ZnSe are given in Fig. 1. One then includes the effect of the damping on the dispersion relation by replacing the right-hand side of Eq. (1) by $\epsilon_R(\omega)$, the real part of the dielectric